Kietäväinen, R., Ahonen, L., Kukkonen, I. T., Niedermann, S., Wiersberg, T. (2014): Noble gas residence times of saline waters within crystalline bedrock, Outokumpu Deep Drill Hole, Finland. - *Geochimica et Cosmochimica Acta*, *145*, p. 159-174.

DOI: http://doi.org/10.1016/j.gca.2014.09.012

Noble gas residence times of saline waters within crystalline bedrock, Outokumpu Deep Drill Hole, Finland

*Riikka Kietäväinen[a], Lasse Ahonen[a], Ilmo T. Kukkonen[a,1], Samuel Niedermann[b] and Thomas Wiersberg[b]

[a]Geological Survey of Finland (GTK), P.O. Box 96, FI-02151 Espoo, Finland
e-mail: riikka.kietavainen@gtk.fi; lasse.ahonen@gtk.fi

[b]Deutsches GeoForschungsZentrum (GFZ), Telegrafenberg, D-14473 Potsdam, Germany
e-mail: nied@gfz-potsdam.de; wiers@gfz-potsdam.de

[1]Present address: Department of Physics, University of Helsinki, P.O. Box 64, FI-00014 Helsinki, Finland
e-mail: ilmo.kukkonen@helsinki.fi

*Corresponding author:
Telephone: +358 (0)50 348 8001

Abstract

Noble gas residence times of saline groundwaters from the 2516 m deep Outokumpu Deep Drill Hole, located within the Precambrian crystalline bedrock of the Fennoscandian Shield in Finland, are presented. The accumulation of radiogenic (^{4}He, ^{40}Ar) and nucleogenic (^{21}Ne) noble gas isotopes *in situ* together with the effects of diffusion are considered. Fluid samples were collected from depths between 180 and 2480 m below surface, allowing us to compare the modelled values with the measured concentrations along a vertical depth profile. The results show that while the concentrations in the upper part are likely affected by diffusion, there is no indication of diffusive loss at or below 500 m depth. Furthermore, no mantle derived gases were found unequivocally. Previous studies have shown that distinct vertical variation occurs both in geochemistry and microbial community structuring along the drill hole, indicating stagnant waters with no significant exchange of fluids between different fracture systems or with surface waters. Therefore *in situ* accumulation is the most plausible model for the determination of noble gas residence times. The results show that the saline groundwaters in Outokumpu are remarkably old, with most of the samples indicating residence times between ~20 and 50 Ma. Although being first order approximations, the ages of the fluids clearly indicate that their formation must predate more recent events, such as Quaternary glaciations. Isolation within the crust since the Eocene –Miocene epochs has also direct implications to the deep biosphere found at Outokumpu. These ecosystems must have been isolated for a long time and thus very likely rely on energy and carbon sources such as H_2 and CO_2 from groundwater and adjacent bedrock rather than from the ground surface.

Keywords: Noble gases, Groundwater, Dating, Crystalline bedrock, Outokumpu

1. Introduction

Within crystalline bedrock, water occupies open space from pores and micro-fractures to major fracture zones which, at least in the uppermost hundreds of meters, forms a relatively continuous network allowing slow circulation of fresh meteoric water. Deep in the bedrock, where both the hydraulic conductivity and the hydraulic head gradient decrease, water becomes typically stagnant. Saline gas-rich groundwaters, characteristically enriched in ^{2}H and ^{18}O compared to meteoric waters, are found worldwide in old crystalline bedrock (e.g. Kloppmann et al. 2002, Frape et al. 2003), including the Fennoscandian Shield in Finland (Nurmi et al. 1988, Blomqvist 1999, Kietäväinen et al. 2013). Several studies have emphasised the importance of low temperature water-rock interaction in the evolution of these waters, and accordingly, very long residence times are supposed to be needed to explain the geochemical and isotopic compositions observed (Fritz and Frape 1982, Frape et al. 1984, Clark and Fritz 1997, Kloppmann et al. 2002, Frape et al. 2003). Findings that microorganisms live in these saline and often gas rich waters (e.g. Haveman et al. 1999, Moser et al. 2003, Itävaara et al. 2011a) have further raised the question of time scales related to rates of microbial metabolism, adequacy of substrates, and biological cycling of elements within the deep subsurface devoid of phototrophic energy (Lin et al. 2006).

A number of methods are available to define a mean residence time of groundwater, many of which are based on radioactive decay, and the age range is ultimately limited by the half life of the decaying element (e.g. Clark and Fritz 1997). Of these, even the ^{36}Cl method with a dating range up to 1.5 Ma has turned out to be insufficient when considering the residence times of saline fluids within the upper continental crust (Louvat et al. 1999, Lippmann et al. 2003). In contrast, methods based on accumulation of radiogenic (^{4}He, ^{40}Ar), nucleogenic (^{21}Ne), and fissiogenic (^{134}Xe, ^{136}Xe) noble gas isotopes in groundwater are not directly limited by a dating range (e.g. Torgersen 1980, Bottomley et al. 1984, Ballentine et al. 1991, Lippmann et al. 2003). The benefits of these methods also include the inertness and well known sources of the nuclides.

Two models are usually applied to calculate the noble gas residence times of groundwaters (e.g. Ballentine et al. 2002). In the *in situ* model the calculation is built on the prerequisite that

(surface driven) water enters a degassed aquifer with zero contribution of radiogenic noble gases. Radiogenic noble gases then accumulate in the groundwater at a rate proportional to their production in the surrounding bedrock. In the flux model, deep crustal flux of noble gases is considered, which may add radiogenic noble gases in excess of *in situ* production. In reality, the situation is hardly ever so straightforward. Instead, fracturing and fluid flow can locally enhance the noble gas flux through the crust (Kulongoski et al. 2005, Torgersen 2010), mixing may take place between different formation waters, or radiogenic noble gases may rapidly be released from fluid inclusions to groundwater. In addition, drilling causes additional mixing of the fluids and adds a drilling fluid component to the system.

Despite these difficulties, the noble gas method is by far the most useful method to determine residence times on the order of millions of years, and based on this method, ancient groundwaters with residence times between millions and hundreds of millions of years have been identified from crystalline bedrock in Canada (Bottomley et al. 1990, Greene et al. 2008), South Africa (Lippmann et al. 2003), and Germany (Lippmann et al. 2005). Recent results from the Timmins mine in Canada have even revealed residence times over 1 Ga for fracture fluids from 2.4 km depth (Holland et al. 2013).

Such studies on residence times of deep groundwaters have so far been almost absent from the Fennoscandian Shield. Noble gas isotopes (only He and Ar) have been previously measured in deep groundwaters of the Fennoscandian Shield by Andrews et al. (1982) from the Stripa mine, by Hilton and Craig (1989) from the Siljan Deep Well (~ 7 km deep), and by Sherwood Lollar et al. (1993) from several sites in Finland, but these studies did either not include absolute noble gas concentration determinations or suffered from disturbed sampling conditions, thus hampering the determination of residence times. Samples from the Stripa mine were later studied for their residence time by Andrews et al. (1989), but without success as the He concentrations were concluded to be controlled by steady state processes. Delos et al. (2010) reported the distribution of helium in groundwaters down to a depth of 1 km in crystalline rock in Sweden (Forsmark and Laxemar) and Finland (Olkiluoto). Based on the observed He concentration gradient within the uppermost bedrock, they derived a deep-source model indicating residence times of tens of millions years. Neretnieks (2013) re-interpreted the data and proposed that the

observed concentration gradient could be due to episodic flushing of water in fractures during the Pleistocene glacial periods. Both these models presume a continuous He concentration gradient reaching much deeper than observations were available (about 1 km), and did not include noble gas isotope data.

The Outokumpu Deep Drill Hole is an uncased, scientific drill hole in eastern Finland (Fig. 1a) and provides direct access to Precambrian crystalline bedrock down to 2516 m depth. The stable isotope composition of water in fluid inclusions suggests that metamorphic fluids do not form a significant groundwater component in Outokumpu (Piribauer et al. 2011). Instead, recharge of meteoric water and subsequent water-rock interaction seem to best explain the observed isotope composition (Kietäväinen et al. 2013). Furthermore, Kietäväinen et al. (2013) suggested that groundwaters in the drill hole were recharged at warmer than present climatic conditions, which would be indicative of residence times on the order of tens of millions of years. Glacial melt waters have been detected elsewhere in the bedrock of Outokumpu (Blomqvist 1999), but not in the Outokumpu Deep Drill Hole (Kietäväinen et al. 2013). Previous studies have revealed diverse microbial communities along the drill hole (Ahonen et al. 2011, Itävaara et al. 2011a, 2011b, Kietäväinen et al. 2013, Purkamo et al. 2013, Nyyssönen et al. 2014).

In this study, noble gases are used to better define the suggested ages of the Outokumpu Deep Drill Hole waters and estimate the time scale required (or available) for the development of saline gas-rich fluids observed in many crystalline terrains. *In situ* accumulation of radiogenic noble gases as well as models including crustal fluxes and diffusion are discussed. In addition to improving our basic understanding on the upper crustal fluids, the information on residence times will potentially be valuable in estimating deep subsurface microbial activity and in assessing the safety of deep geological disposal of nuclear waste and other operations exploiting crystalline bedrock environments.

2. Study site

The 2516 m deep Outokumpu Deep Drill Hole is located in eastern Finland within the Fennoscandian Shield (Fig. 1a). Situated at the NW-SE trending boundary between the Archaean

and Proterozoic domains of the shield, the Outokumpu area is characterised by a complex geological history, including the formation of world class Cu-Zn-Co ore deposits (e.g. Peltonen et al. 2008). Due to tectonic thickening and magmatic under- and intraplating during the Svecofennian orogeny (1.9 – 1.8 Ga), unusually thick crust up to 65 km is found at the Archaean-Proterozoic boundary (Korsman et al. 1999).

The bedrock of the study site consists of 1.96-1.90 Ga mica schist, black schist and ophiolitic rocks (Outokumpu assemblage) overlying the Archaean basement, and is dissected by 1.86 Ga granitoids (Huhma 1986, Claesson et al. 1993, Peltonen et al. 2008, Lahtinen et al. 2010) (Fig. 1). After the main regional deformation, metamorphic conditions reached their peak in the study area at middle amphibolite facies (550 – 675ºC at 3 – 5 kbar) at 1.885 Ga (Korsman et al. 1999, Säntti et al. 2006). The main tectonic feature in the area is the SE dipping Outokumpu fault (Fig. 1a), which reaches the surface 3 km NW of the Outokumpu Deep Drill Hole and probably dissects the crust at 3 – 4 km depth below the deep drill hole site (Kukkonen et al. 2012). Tectonic activity has long since ceased, although minor movements related to glacial depression and post-glacial uplift may have occurred during the last 2 million years of glaciations and deglaciations (e.g. Steffen and Wu 2011). The present erosional level was reached at the latest by the beginning of the Cambrian at ca. 600 Ma (Kohonen and Rämö 2005). At present, over 30 m of Quaternary sand and silt covers the bedrock at the study site.

Petrophysical measurements of rock density and effective porosity from the Outokumpu Deep Drill Core are given in Table 1. In addition to pore spaces, fractures of different scale from micro-fractures to major fracture zones occur in crystalline bedrock. The major fracture zones in the Outokumpu Deep Drill Hole, as indicated by borehole loggings, are shown in Figure 1b. Based on reflection seismics, structures including the fracture zone at 970 m are mainly horizontal to subhorizontal in character (Heinonen et al. 2011). Due to the low geothermal gradient, the bottom hole temperature only reaches 40°C (Kukkonen et al. 2011).

Formation waters of the Outokumpu Deep Drill Hole are characteristically rich in dissolved CH_4, N_2, H_2 and He and have high salinity up to 70 g l^{-1} (Kietäväinen et al. 2013 and this study). Previous studies have also shown that distinct vertical variation in water geochemistry occurs

along the drill hole, indicating stagnant waters with no significant exchange of fluids between different fracture systems or with surface waters. Hydraulic tests performed during and after the drilling as well as temperature logs mostly indicate negligible fluid flow in the bedrock (Fig 1b; Ahonen et al. 2011, Kukkonen et al. 2011). Based on Sr and water stable isotopes and overall geochemistry, five different water types have been discerned within the drill hole, with a major divide in composition at around 1300 m depth (Fig. 1b; Kietäväinen et al. 2013).

Variable microbial communities, including methanogenic archaea and sulphate reducing bacteria, inhabit the fracture fluids (Itävaara et al. 2011a, 2011b, Purkamo et al. 2013, Nyyssönen et al. 2014). The bacterial community structuring has been found to correlate with the different water types (Kietäväinen et al. 2013, Nyyssönen et al. 2014), further emphasising the isolated and stratified nature of the fluids.

3. Material and methods

3.1 Samples

Two methods were utilised to collect groundwater samples for noble gas analysis from the Outokumpu Deep Drill Hole. In the first instance, samples were taken in connection with the tube sampling in May 2011. In this method, modified after Nurmi and Kukkonen (1986), Cu-tubes were attached between 100 m sections of polyamide tubes equipped with a back pressure valve at the end and shut off valves between each 100 m section. The tube sampler was slowly lowered into the drill hole until the end of the tube reached 2450 m depth, and then lifted up. The valves were closed as soon as they reached the surface and the Cu-tubes were immediately sealed with clamps. In total, three Cu-tube samples (from 850, 1650, and 2350 m) were taken with this method, and are hereafter referred to as “Cu-tube water”. Later it was noticed that the clamps of the 850 m sample were not tight, and therefore we excluded this sample from the analysis.

In August 2011, eight samples were collected using a Leutert Positive Displacement Sampler (PDS), covering a depth range from 500 m to 2480 m. In contrast to the tube sampling method,

214 the PDS method allows sampling at *in situ* pressures, thus minimising fractionation related to
215 potential degassing during sampling. Furthermore, the gas/water ratio can be reliably determined
216 (Regenspurg et al. 2010). The samples were transferred from the down hole sampler into a
217 transfer vessel and split into water and gas phases in an evacuated sampling line connected with
218 a Cu-tube and a gas sampling bulb made of glass. Gas separation was assisted with a heated
219 ultrasonic bath and the Cu-tubes (hereafter referred to as "Cu-tube gas") were cold welded with
220 clamps after ca. 10 minutes of degassing. Gas/water ratios were determined based on pressure
221 build-up in the sampling line during degassing. The final pressure inside the containers varied
222 from 187 mbar to 1240 mbar. In order to increase the pressure inside the gas sampling bulbs to
223 atmospheric (1012 mbar at the time of sampling), deionised and degassed water was added into
224 glass bulbs containing the samples OUTO-1470-2 and OUTO-2480 after the Cu-tube gas
225 samples had been taken.
226
227 *3.2 Analytical methods*
228
229 Relative gas concentrations (including He, Ar, CO_2, O_2, N_2, H_2 and CH_4) of the sampling bulb
230 gas samples were determined in the field by a Pfeiffer GSD 300 OmniStar quadrupole mass
231 spectrometer (QMS) using Quadstar 32-bit software. The same samples were later analysed by
232 gas chromatography (GC) at Ramboll Analytics (Vantaa, Finland) (Kietäväinen et al. 2013). The
233 relative uncertainty of the GC analysis, including both analytical uncertainty and reproducibility
234 of the duplicates, was 19 % for He and 31 % for Ar at 2σ level. Independent of the gas species,
235 the reproducibility of QMS measurements is 2% for the measured concentrations which were all
236 >100 ppmv. Including the uncertainty of the calibration measurement, we estimate the total
237 analytical uncertainty of the QMS measurements to be twice as high, i.e. 4 % for all gas species.
238
239 The isotope compositions of noble gases were determined with a VG 5400 mass spectrometer
240 equipped with both Faraday and electron multiplier detectors at GFZ Potsdam, Germany. All
241 three types of samples were analysed: water in a Cu-tube, gas in a Cu-tube, and gas in a sampling
242 bulb. Due to high pressure inside the Cu-tube water samples, spontaneous degassing generally
243 provided abundant gas for the analysis. Only the sample OK-24/25 was actively degassed in an
244 ultrasonic bath for a second run after a first measurement of the free gas phase. Purification of

noble gases was performed in a line consisting of a cold trap (-79°C), two Ti sponge-getters (+400°C) and two Zr-Al (SAES) getters (+250°C and room temperature). In addition, activated charcoal cooled with liquid nitrogen (-196°C) was used to enhance purification during the He and Ne measurements. Ar, Kr, and Xe were adsorbed to a stainless steel frit in a cryostatic cold head at 50 K, and He and Ne to activated charcoal in another cold head at 11 K. Each noble gas was then released and measured separately by sequentially heating the first cold head to 80 K, 100 K, and 150 K to release Ar, Kr and Xe, and the second cold head to 35 K and 120 K to release He and Ne, respectively. The system was calibrated and the reproducibility of the analysis tested by analysing an artificial gas mixture of known composition and isotope ratios. Further details on analytical procedures and data reduction methods can be found in Niedermann et al. (1997).

4. Results

4.1 Gas concentrations

The results of gas chromatography (GC), together with the isotopic (δ^2H, δ^{18}O, ^{87}Sr/^{86}Sr) and general geochemical composition of the water samples, have been previously reported by Kietäväinen et al. (2013). The present study is based on the results of quadrupole mass spectrometric (QMS) analyses conducted at the time of sampling and noble gas mass spectrometry (NGMS) conducted approximately half a year later.

Oxygen was present in all the samples, ranging between 0.08 and 2.6 vol % in the QMS (Table 2) and 0.07 and 5.8 vol % in the GC analyses. Such amounts of free molecular oxygen are however unlikely to be found deep underground, and have not been detected during long term on-line monitoring of the pumped fluid in Outokumpu (Purkamo et al. 2013). Therefore we consider oxygen to be a contaminant derived from air. Due to the high He and low Ar concentrations in the samples compared to air, air contamination is more prominent for Ar than for He. It was observed that, even taking account of the error limits, He/Ar ratios were progressively lowered between the QMS, GC and the mass spectrometric analysis of noble gases. This suggests that air was leaking in (and perhaps He leaking out) not only during

sampling but also during sample storage. Therefore the QMS results are thought to best represent the original concentrations in groundwater and have been used in the residence time calculations.

The measured gas concentrations (X in vol %) were corrected for contamination by assuming that the contaminant is of atmospheric origin:

$$X_{corrected} = X_{measured} - \left(\frac{O_{2\,measured}}{O_{2\,air}} \cdot X_{air}\right) \quad (1)$$

The atmospheric volume fractions as measured with the QMS at Outokumpu were used for X_{air} (O_2, 20.95 %; N_2, 78.085 %; Ar, 0.93 %; CO_2, 0.039 %; He, 0.000524 %; CH_4, 0.00015 %, H_2, 0.00014 %). Subsequently, the absolute gas concentrations were determined from air-corrected relative volume data by using the measured gas/water ratios:

$$[X] = \left(\frac{X_{corrected}}{100}\right) \cdot gas/water \quad (2)$$

where [X] is the concentration of a gas X in $cm^3\ g^{-1}$ at standard temperature and pressure (STP). The corrected values were not normalised to 100 % prior to the calculation (Eq. 2), as it was assumed that air contributed to the gas phase already during sampling, i.e. increased the gas/water ratio. As gas/water ratios of the Cu-tube water samples were not known, absolute concentrations could not be determined for them.

The air-corrected concentrations of gases are given in Table 2. No systematic change is observed in the noble gas concentrations with depth. Both He and Ar concentrations are highest at 970 m depth, whereas a concentration minimum is seen at 1470 m for Ar and 2350 m for He (Fig. 2a and 2b).

4.2 Noble gas isotopes

The measured isotopic ratios of noble gases in the Outokumpu Deep Drill Hole samples are given in Table 3. The $^3He/^4He$ ratio is rather constant throughout the drill hole profile (Fig. 2c).

306 Both the $^{20}Ne/^{22}Ne$ and $^{21}Ne/^{22}Ne$ ratios are close to atmospheric and distinguishable ^{21}Ne
307 excesses are observed only in the gas sampling bulb samples from 970 m and 1470 m and in the
308 two Cu-tube water samples from 1650 m and 2350 m. Likewise, the highest $^{40}Ar/^{36}Ar$ ratios are
309 found in these samples (Fig. 2d), indicating minimal air contamination compared to the Cu-tube
310 gas samples, as also inferred by high $^{4}He/^{20}Ne$ ratios (Table 3). Differences between the Cu-tube
311 and gas sampling bulb samples, collected at the same time, are likely related to leakage of air and
312 mass fractionation as discussed in more detail in section 5.2. Higher than atmospheric ratios of
313 $^{134}Xe/^{132}Xe$ and $^{136}Xe/^{132}Xe$ are found at the two deepest sampling depths whereas most other Xe
314 ratios are atmospheric within uncertainties. Together with the high uncertainty of absolute
315 concentrations of Xe, this precludes the use of Xe in residence time calculations.
316
317 **5. Discussion**
318
319 *5.1 Mantle, crustal and air-derived noble gas components*
320
321 The noble gas concentrations (C_{tot}) are a sum of components derived from different sources
322 including air (solution equilibrium and excess air components as well as possible contamination),
323 mantle, and crust (e.g. Kipfer et al. 2002). In order to determine noble gas residence times, the
324 concentrations of radiogenic (or nucleogenic) nuclides formed within the crust need to be
325 resolved. Different components can be determined based on the defined end member isotopic
326 ratios for each noble gas (Ballentine et al. 2002). The contribution of the mantle component is
327 most readily determined with He.
328
329 The $^{3}He/^{4}He$ ratios of the Outokumpu Deep Drill Hole fluid samples are all within the typical
330 range for crustal He of up to ~$3 \cdot 10^{-8}$ (Ballentine and Burnard 2002), and clearly differ from the
331 $^{3}He/^{4}He$ value of $8.69 \cdot 10^{-6}$ reported for the subcontinental lithospheric mantle (i.e. $^{4}He/^{3}He$ =
332 115,000; Gautheron et al. 2005). This is in accordance with the unlikely presence of a mantle
333 component in an area of an over-thickened crust. Therefore we consider the noble gases to be
334 composed of only two components:
335
336 $$C_{tot} = C_{air} + C_{crust} \quad (3)$$

Based on the $^{3}He/^{4}He$ and $^{4}He/^{20}Ne$ ratios (Table 3), virtually all He is radiogenic and the air-corrected $[He]_{tot}$ (Table 2) thus equals $[^{4}He]_{crust}$ and can be directly used in residence time calculations. Besides air-contamination, a significant part of Ne and Ar may comprise dissolved or excess air. Therefore, another approach is needed to obtain C_{crust} for them. At first the concentrations of $[^{21}Ne]_{tot}$ and $[^{40}Ar]_{tot}$ were determined based on their partial pressures relative to He as exemplified here for ^{21}Ne:

$$[^{21}Ne]_{tot} = p_{21Ne}/p_{4He} \cdot [^{4}He]_{tot} \quad (4)$$

where p_{21Ne} and p_{4He} are partial pressures of ^{21}Ne and ^{4}He determined during the noble gas mass spectrometric measurement. Subsequently, the concentrations of crustal ^{21}Ne and ^{40}Ar (Table 3) were determined according to the equations (5) and (6) (Ballentine et al. 2002), with the atmospheric ratios of 0.00296 for $(^{21}Ne/^{20}Ne)_{air}$ (Eberhardt et al. 1965) and 298.56 for $(^{40}Ar/^{36}Ar)_{air}$ (Lee et al. 2006).

$$[^{21}Ne_{nucl}] = [^{21}Ne_{tot}] \cdot [1-(^{21}Ne/^{20}Ne)_{air}/(^{21}Ne/^{20}Ne)_{measured}] \quad (5)$$

$$[^{40}Ar_{rad}] = [^{40}Ar_{tot}] \cdot [1-(^{40}Ar/^{36}Ar)_{air}/(^{40}Ar/^{36}Ar)_{measured}] \quad (6)$$

As the He/Ne and He/Ar ratios had changed during sample storage (i.e. after the $[^{4}He]_{tot}$ was measured), an assumption is made that only addition of air, but no loss of crustal ^{21}Ne or ^{40}Ar occurred.

5.2 Mass fractionation

If mass fractionation has taken place, the measured noble gas concentrations may no more represent original concentrations in groundwater. Therefore it is essential to either try to correct for such fractionation or exclude the affected samples from residence time calculations. Elemental fractionation of noble gases is ultimately driven by the difference in their masses and may take place for example during degassing or dissolution (Ballentine et al. 2002). Degassing is unquestionably taking place at the Outokumpu Deep Drill Hole, where continuous bubbling of

368 gases is observed at the well head. This process is, however, potentially affecting only the
369 topmost part of the drill hole. Based on concentration and solubility data, no spontaneous
370 degassing should take place below 150 m, i.e. at the depths in target of this study. Temporary
371 disturbance may have been caused by pumping experiments, conducted at several depths during
372 the existence of the drill hole, and by the drilling operation itself. Due to a slight decrease in
373 pressure during sampling, the tube sampler is also potentially prone to partial degassing of the
374 samples. If there is no degassing, or the water is completely degassed (as was the aim during the
375 transfer from the PDS into the sample containers), no fractionation should occur.
376
377 If driven by diffusion, elemental fractionation may be accompanied by isotopic fractionation
378 (Ballentine et al. 2002). The most extensive fractionation is related to Rayleigh distillation type
379 processes, as exemplified for partial degassing (e.g. Ballentine et al. 2002, Matsumoto et al.
380 2004):
381
382 $$({}^{i}X/{}^{j}X)_{degassed} = ({}^{i}X/{}^{j}X)_{original} \cdot \frac{1-f^{\alpha}}{1-f} \quad (7)$$
383
384 where ${}^{i}X/{}^{j}X$ is the ratio of two isotopes (for example ${}^{20}Ne/{}^{22}Ne$) in the dissolved phase prior to
385 (*original*) and in the gas phase after partial degassing (*degassed*), f is the fraction of gas retained
386 in the water, and α is the fractionation factor. For diffusion-controlled fractionation, the latter is
387 commonly determined as a square root relation of the two masses (e.g. Marty 1984, Ballentine et
388 al. 2002):
389
390 $$\alpha = \sqrt{m_j/m_i} \quad (8)$$
391
392 For example, α for the fractionation between ${}^{20}Ne$ and ${}^{22}Ne$ is therefore $\sqrt{22/20} \approx 1.05$.
393
394 Free-molecule diffusion, analogous to partial degassing, may also happen when gas is passing
395 through a conduit with a diameter smaller than the mean free path of the gas atoms (Marty 1984,
396 Ballentine et al. 2002). If air is leaking through such conduits during sample storage, this effect

may cause fractionation of gaseous samples even if complete degassing had been achieved during sampling.

Based on equations (7) and (8) the relative effect of fractionation on different isotope ratios can be calculated and used to interpret isotopic fractionation within a sample set. A three-isotope plot of neon is presented in Figure 3 for the Outokumpu Deep Drill Hole samples. From Fig. 3, it can be seen that the sampling bulb gas samples show Ne isotopic compositions indicative of mixing between atmospheric and crustal Ne, whereas the Cu-tube gas samples have been affected by isotopic fractionation, as indicated by the alignment of data along the mass fractionation line (MFL in Fig. 3). As both types of samples have been collected from the same sampling line, fractionation must have happened during sample storage or analysis. This fractionation is also evident in the $^{38}Ar/^{36}Ar$ ratios (Table 3), and is most likely related to preferential leakage of lighter isotopes from air into the low-pressure samples.

As the degree of fractionation increases with relative difference of mass (Eq. 8), it will be largest for $^{3}He/^{4}He$ and smallest for $^{134}Xe/^{132}Xe$. The effect on the ^{4}He age will, however, be negligible because of the huge difference between the atmospheric and measured $^{3}He/^{4}He$ ratios. Likewise, the effect on $^{40}Ar_{rad}$ will be minor. However, Ne is much more affected, and the isotope ratio data of samples plotting on the MFL in Fig. 3 cannot be used to calculate crustal ^{21}Ne concentrations. The two Cu-tube water samples (OK-17/18 and OK-24/25/B) also deviate from the typical air-crust mixing line in the Ne three-isotope plot (Fig. 3). Since a mantle component can be excluded based on the crustal $^{3}He/^{4}He$ ratios within the range of $1\text{-}2 \cdot 10^{-8}$ (Table 3), it cannot explain the shift. Interestingly, similar nucleogenic Ne compositions enriched in ^{21}Ne over ^{22}Ne have been found in deep, saline fracture waters of the Witwatersrand gold mines in South Africa (Type B fluid of Lippmann-Pipke et al. 2011) and the Timmins mine in Canada (Holland et al. 2013). Comparable to the deepest parts of the Outokumpu Deep Drill Hole, this Ne anomaly is featured by fluids typically enriched in H_2 and hydrocarbons of potentially abiotic origin and was suggested to represent an Archaean fluid component (Lippmann-Pipke et al. 2011).

5.3 Mixing

Mixing between a younger and an older component cannot be discerned from *in situ* accumulation of radiogenic components (i.e. the constant aging of groundwater) by the noble gas method. Fortunately there are other parameters such as Sr isotopes and relations of salinity to water stable isotopes which can be used to estimate mixing. Accordingly, Kietäväinen et al. (2013) concluded that even though groundwater mixing has occurred due to drilling and sampling operations in the Outokumpu Deep Drill Hole, geochemically and isotopically distinct water types are still evident. Stagnant water types also indicate negligible vertical fluid flow in the bedrock. Around 2260 m depth, however, mixing of formation water with up to 30 % of fresh drilling fluid was observed (Kietäväinen et al. 2013). Consequently the radiogenic He concentrations as well as the resulting residence times are likely too low at 2350 m depth, while at the same time excess (atmospheric) Ar may have been added and $^{40}Ar/^{36}Ar$ ratios lowered.

5.4 In situ noble gas residence times

The *in situ* accumulation rate of radiogenic nuclides (J_i) within an aquifer depends on the production rate of these nuclides in the aquifer rock matrix and on the physical properties of the aquifer (e.g. Torgersen 1980):

$$J_i = \Lambda \cdot \left[\frac{1-\theta}{\theta}\right] \cdot \left(\frac{\rho_r}{\rho_w}\right) \cdot P_i \quad (9)$$

where Λ is a release coefficient, θ is the fractional effective porosity of the rock, ρ_r and ρ_w are the densities of the rock and water (with ρ_w assumed to equal 1 for all samples), respectively, and P_i is the production rate of the nuclide (*i*) in question. Λ is a measure of the proportion of gas released into the water, and is here assumed to be 1 (i.e. 100 %) for all noble gases. The following equations, with decay constants and isotopic ratios according to Steiger and Jäger (1977), are used to calculate the P_i values (in cm^3 STP g^{-1} a^{-1}):

$$P_{4He} = 1.207 \cdot 10^{-13}[U] + 2.867 \cdot 10^{-14}[Th] \quad (10)$$

$$P_{21Ne} = 5.432 \cdot 10^{-21}[U] + 1.290 \cdot 10^{-21}[Th] \quad (11)$$

$$P_{40Ar} = 3.885 \cdot 10^{-14}[K] \quad (12)$$

where [U] and [Th] are the concentrations in ppm, and [K] is the concentration in % (Ballentine et al. 1991, Lippmann et al. 2003). The $^{21}Ne/^{4}He$ production ratio of $4.5 \cdot 10^{-8}$ from Yatsevitch and Honda (1997) was used to obtain the coefficients in Eq. (11) from Eq. (10). Parameters used to calculate *in situ* accumulation rates in Outokumpu are given in Table 1 and are based on hundreds of measurements from the Outokumpu deep drill core by Airo et al. (2011) and Västi (2011). Even though the Outokumpu assemblage, consisting of e.g. serpentinite and black schist, is a rather heterogeneous unit both in terms of porosity and geochemistry, altogether variation is small and therefore the average of all measurements (the lowest row in Table 1) has been used in the calculations. An error representative of two standard deviations of the mean of each parameter (Table 1) has been included in the cumulative error calculation of model ages. For porosity, in particular, the error is likely to be higher, because of difficulties of a reliable determination of bedrock porosity from drill core samples and large variations between different parts of the fractured bedrock. Due to locally increased porosity in fracture zones, the use of effective porosity of drill core samples is thus a minimum estimate of total porosity and could possibly result in too low model ages. For instance, with other parameters staying constant, doubling the porosity will approximately double the calculated residence times.

If *in situ* production is considered the only source for radiogenic ^{4}He, then the residence time $\tau_{in\ situ}$ can be simply calculated by dividing the resolved crustal ^{4}He concentration (Eq. 2) by the *in situ* accumulation rate of radiogenic He (Eq. 9) (Torgersen 1980):

$$\tau_{in\ situ} = [^{4}He_{crust}]/J_{4He} \quad (13)$$

By analogy, concentrations of crustal ^{21}Ne and ^{40}Ar can be used together with their accumulation rates (Eq. 9) to determine *in situ* model ages.

In situ model ages from 17 (±4) to 58 (±14) Ma are indicated by ^{4}He, 15 (±6) and 45 (±22) Ma by ^{21}Ne and from 4.1 (±0.9) to 22 (±3) Ma by ^{40}Ar (Table 4, Fig. 4). Altogether, most of the samples indicate isolation of these groundwaters from the meteoric water cycle since the Eocene - Miocene epochs.

In reality, a release of 100 % of the noble gases produced within the host rock, as assumed in the residence time calculations, is not necessarily met in nature. While He, although depending on the effective grain size, easily moves into groundwater (Torgersen and Clarke 1985, Drescher et al. 1998), Ar is not readily released from minerals at low temperatures (Ballentine et al. 1994, Tolstikhin et al. 1996). The release of Ar into groundwater is most likely dominated by water-rock reactions (Tolstikhin et al. 1996) and could therefore be very variable, as observed by Drescher et al. (1998) in their study of noble gases in metamorphic rocks from the KTB deep drill site in Germany. A lower than supposed release factor may explain discrepancies between the He and Ar based residence times. In addition, due to the greater sensitivity of Ar and Ne to air contamination compared to He, mixing with air or recent fluid (drilling water) may have affected the Ar and Ne results by lowering the isotopic ratios which were used to calculate $[^{21}Ne_{nucl}]$ and $[^{40}Ar_{rad}]$ (Eqs. 5 and 6) and the ^{4}He based ages may be the most reliable ones.

5.5 Diffusion and crustal scale flux

It is largely accepted that atmospheric loss of ^{4}He into space is compensated by degassing of the Earth's crust. However, the extent of crustal scale flux has been long debated, and data from various locations indicate that at least large variations can occur (Torgersen 1989, 2010). Observations from sedimentary basins, confined aquifers in particular, have shown that incoming fluxes could be of importance in adding noble gases in excess of the *in situ* production (Torgersen and Clarke 1985, Torgersen and Ivey 1985). The generally more uniform diffusion properties of crystalline bedrock, combined with substantial production of noble gases within the formation, are not likely to favour such accumulation of crustal flux. Rather, the observed crustal flux from the Precambrian Shield in Canada ($5.4 \cdot 10^{-6}$ cm^3 STP ^{4}He cm^{-2} a^{-1}, i.e. $4.57 \cdot 10^{10}$ ^{4}He atoms m^{-2} s^{-1}), which is based on data collected from small lakes by Clarke et al. (1977, 1983) and Top and Clarke (1981), is consistent with the theoretical value for steady state degassing of the continental crust (Torgersen 2010). Crustal fluxes of the heavier noble gases are less well constrained (Drescher et al. 1998, Torgersen 2010).

A concentration gradient is needed as a driving force for diffusive flux. Due to continual production of noble gases in the crust, such a gradient is formed close to the atmospheric

boundary (z = 0). Considering 1-D diffusion (along depth z), the concentration (C) of a diffusing gas in a unit volume changes with time (t) due to *in situ* accumulation (J_i) and due to diffusion (D) through the unit volume along a changing concentration gradient (Andrews 1985):

$$\partial C/\partial t = J_i + D(\partial^2 C/\partial z^2) \quad (14)$$

Assuming a constant production rate and diffusion coefficient for all values of z, zero concentration for all z at t = 0, zero concentration for all t at z = 0, and a concentration gradient approaching zero at $z \rightarrow \infty$, an exact solution of the one-dimensional diffusion equation can be derived (Andrews 1985). The exact solution of Eq. (14) can be approximated by the following equation given by Andrews (1985):

$$C(z,t) = J_i t \cdot [1 - e^{\{-2\pi^{-0.5} \cdot z \cdot (Dt)^{-0.5}\}}] \quad (15)$$

Figure 5 shows the modelled diffusion profiles (Eq. 15) for He in crystalline bedrock with a porosity of 0.5 % and U and Th concentrations of 6 and 9 ppm, i.e. average values for the bedrock in Outokumpu (Table 1). Based on experimental determinations from granitic rocks (Altman et al. 2004, Neretnieks 2013), the effective diffusion coefficient was set to $3.18 \cdot 10^{-9}$ $cm^2\ s^{-1}$ (i.e. $1 \cdot 10^{-5}$ $m^2\ a^{-1}$). According to the model, diffusive loss into the atmosphere creates a linear decrease of the concentration of the diffusing gas towards the surface. Through time, the diffusive front progresses and reaches deeper levels of the crust. As the time needed for different noble gas fluxes to reach steady state is directly proportional to the difference between their diffusion coefficients (Castro et al. 1998), this would take much longer for Ne and Ar than He, and even longer for Xe. As long as the diffusive loss does not equal the *in situ* production at a given depth, accumulation of noble gases will take place.

The measured He concentrations from the Outokumpu Deep Drill Hole plot around the 30 Ma diffusion curve, which does not show diffusive loss at or below 500 m depth (Fig. 5). In addition to the PDS samples from 2011, the average of three samples from 180 m depth taken with a pressurised sampling device (PAVE) in 2012 after 45 days of pumping between packers, and one sample taken already during drilling in 2004 from around 977 m depth (Ahonen et al. 2011) are

552 shown. Our observation of the absence of a helium concentration gradient deep in the bedrock is
553 complementary to that reported by Delos et al. (2010) and Neretnieks (2013) for the upper 1000
554 m, where a distinct gradient exists. The diffusive front has likely reached the 180 m depth, but it
555 would take tens of millions of years before a diffusive gradient could develop at depths greater
556 than a few hundred metres. Thus, by comparing the diffusion model to observed noble gas
557 concentrations, we can conclude that crustal scale diffusion is not likely to affect noble gas
558 concentrations of groundwater at or below 500 m depth in Outokumpu, and thus the use of the *in*
559 *situ* model in calculating residence times at about 500 m and below is justified.
560
561 *5.6 On the origin and evolution of deep fracture fluids in Outokumpu*
562
563 Characteristic features of the deep groundwaters in the Outokumpu Deep Drill Hole, common to
564 deep fracture fluids of old shields in all over the world, include high salinity, high amounts of
565 dissolved gases with non-atmospheric composition, and water stable isotopic compositions
566 shifted above the meteoric water line (Ahonen et al. 2011, Kietäväinen et al. 2013). However,
567 not much is known about the conditions in which they formed and the processes behind their
568 distinct compositions (e.g. Frape et al. 2003).
569
570 Our results on noble gas residence times in the Outokumpu Deep Drill hole indicate isolation of
571 these waters from the near surface hydrological circulation since the Eocene – Miocene epochs.
572 This is similar to the results from Olkiluoto in south-west Finland, where a noble gas residence
573 time of 35 Ma has been indicated by the absolute He concentrations in groundwaters below 250
574 m depth (Delos et al. 2010). Despite the slightly different hydrogeological history of the
575 presently coastal Olkiluoto and inland Outokumpu (99 m above sea level), both sites are
576 characterised by Palaeoproterozoic bedrock with brackish to saline fracture fluids and abundant
577 dissolved gases. In Olkiluoto, Neretnieks (2013) favoured a scenario according to which matrix
578 pore water was episodically flushed by glacial melt water, resulting in a mixed age. The lack of a
579 glacial melt water component in the Outokumpu Deep Drill Hole does not seem to support this
580 kind of hypothesis in our case, unless the change in the isotopic composition of water took place
581 much faster than in some other locations (e.g. elsewhere in Outokumpu; Blomqvist 1999) where
582 such a component has been identified.

583

584 Let us assume that the measured concentrations and therefore the calculated residence times truly
585 represent *in situ* ages of these waters. In what conditions may the groundwater recharge have
586 taken place? The Tertiary of Finland is poorly known, because of the weak preservation of the
587 geological record in the glaciated landscape. The occurrence of Tertiary marine microfossils in
588 northern Finland has led to the interpretation that vast areas of northern Finland were below sea
589 level during the Eocene (Tynni 1982). However, this view has been challenged by Hall and Ebert
590 (2013), who suggested that the diatoms in these sediments originate from a distant source and
591 have been deposited by wind. Recent oxygen and hydrogen isotope determinations from rare
592 kaolin deposits in Finland indicate formation by weathering at temperatures between 13 and 15
593 °C, i.e. likely during the Palaeocene to Eocene or the Late Oligocene to Middle Miocene, and
594 consequently do not support marine transgression at that time (Gilg et al. 2013). Due to humid
595 climate that has supposedly prevailed in northern latitudes within this period (Greenwood et al.
596 2010, Larsson et al. 2011), the conditions may have been favourable not only for the formation
597 of the kaolinites but also for groundwater recharge. The Cenozoic uplift of Fennoscandia (Anell
598 et al. 2009) could have further assisted the preservation and isolation of these groundwaters in
599 the bedrock.

600

601 Using the silicate hydration hypothesis (e.g. Fritz and Frape 1982, Kloppmann et al. 2002) to
602 model the evolution of the isotopic composition (δ^2H, $\delta^{18}O$) of groundwater in Outokumpu,
603 Kietäväinen et al. (2013) suggested that recharge occurred during climatic conditions 3 - 10°C
604 warmer than at present. Temperature dependency of the solubility of atmospheric noble gases in
605 water has been used in several studies to determine recharge temperatures of groundwaters (e.g.
606 Aeschbach-Hertig et al. 2002, Kipfer et al. 2002). Due to the lack of absolute concentrations of
607 heavier noble gases, our data set cannot be used for this purpose. However, from the residence
608 time perspective it can be noted that based on the reconstruction of temperatures from $\delta^{18}O$ of
609 deep sea foraminifera, climate has significantly cooled since the Early Eocene climatic optimum
610 around 50 Ma (Zachos et al. 2001), while since that time the palaeolatitude of Fennoscandia has
611 increased by about 8° (Torsvik et al. 2001). As such, our results on noble gas residence times on
612 the order of tens of millions of years are congruent with the warmer climate scenario suggested
613 in Kietäväinen et al. (2013).

In any case, the results from Finland are within the supposed age range of similar groundwaters in Canada, South Africa and Sweden (Lippmann et al. 2003, Greene et al. 2008, Delos et al. 2010). Whether the similar residence times indicate some major geological circumstance, a similar geochemical evolution or are just coincidental remains an open question.

5.7 *Implications for the deep biosphere*

Isolation of the Outokumpu Deep Drill Hole groundwater within the crust since the Eocene – Miocene epochs has also direct implications for the deep biosphere within the fractured bedrock. These ecosystems must have been isolated for a long time and thus very likely rely on energy and carbon sources such as H_2 and CO_2 from groundwater and adjacent bedrock rather than from the ground surface. As inert species, noble gases cannot be utilised by microorganisms and could therefore be potentially used to estimate microbial consumption of other, co-existing crustal gases such as CH_4, CO_2 and H_2: if notable consumption of other gases is to happen, while accumulation of noble gases takes place, this may appear as a negative correlation of concentrations.

In the Outokumpu Deep Drill Hole the concentration of He, and to a lesser extent also Ar, correlates positively with all other gases measured except for H_2 and CO_2; instead, the highest concentration of He is found where the concentrations of H_2 and CO_2 are lowest. A possible explanation for this inverse correlation is that H_2 and CO_2 are, and have been, consumed by microorganisms. Potential for both autotrophic acetate production and methanogenesis utilising these substrates has been detected in metagenomic sequencing of the Outokumpu samples (Nyyssönen et al. 2014). An isotopic study of hydrocarbons, dissolved inorganic carbon, and H_2 is under way to better resolve the questions related to the origin and possible consumption of these gases in the deep crystalline rock environment.

6. Conclusions

644 The noble gas composition of saline fluids down to 2480 m depth within the Outokumpu Deep
645 Drill Hole was studied. No mantle derived gases were found unequivocally. The presence of
646 radiogenic nuclides of He and Ar as well as nucleogenic ^{21}Ne enabled noble gas residence times
647 to be determined. Our He concentration data from 500 – 2500 m do not show any observable
648 concentration gradient, indicating that this depth range is neither affected by diffusion flux
649 towards the surface nor has been subjected to any major convective flushing effects. Therefore *in*
650 *situ* accumulation could be assumed as a basis for the calculations.
651
652 Our estimations of residence times are based on the average U, Th and K concentrations and
653 effective porosity determined form the Outokumpu Deep Drill Core. The complete release of
654 radiogenic noble gases into the water phase was assumed. In general, residence times between 17
655 and 58 Ma are indicated by ^{4}He and are in good agreement with ^{21}Ne based ages, while
656 somewhat younger ages between 4 and 22 Ma were obtained by using the accumulation of ^{40}Ar.
657 Systematic difference between the ^{4}He and ^{40}Ar ages of water can be explained by their different
658 release factors: more Ar remains trapped in the mineral lattice compared to the more mobile He,
659 while neon evidently has intermediate properties in terms of molecular mobility. Congruent
660 residence times are obtained if the release factors for ^{21}Ne and ^{40}Ar are set to more realistic
661 values below 1. In addition, mixing with fresh drilling fluid may have lowered the $^{40}Ar/^{36}Ar$
662 ratios and may consequently partly explain the lower ^{40}Ar residence times.
663
664 Although being first order approximations, the ages obtained in this study confirm that the
665 isolated fluids in Outokumpu are ancient, and not related to more recent events, such as
666 Quaternary glaciations. Instead, humid climate and regional uplift during the Tertiary may have
667 favoured the formation and isolation of these groundwaters. Our results on noble gas residence
668 times have also direct implications for the deep biosphere ecosystems discovered in the
669 Outokumpu Deep Drill Hole. These ecosystems must be remarkably old, and further, they very
670 probably rely on energy and carbon sources from the bedrock rather than the ground surface.
671
672 **Acknowledgements**
673

674 The PDS sampling at the Outokumpu Deep Drill Hole would not have been possible without the
675 ICDP Operational Support Group. Valuable assistance in the field was given by Arto Pullinen
676 from the Geological Survey of Finland. Enzio Schnabel from the GFZ Potsdam is acknowledged
677 for the skilled assistance in the noble gas laboratory. Co-operation with the molecular biology
678 research group led by Merja Itävaara from the Technical Research Centre of Finland has greatly
679 helped to understand the deep microbial world. Juha Karhu and Nina Heikkinen from the
680 University of Helsinki also contributed to this study. The manuscript benefited substantially from
681 critical comments from the Associate Editor Pete Burnard and three anonymous reviewers. This
682 study was supported by the Academy of Finland DEEP LIFE project (Grant 133348/2009), the
683 Finnish Research Program on Nuclear Waste Management (Grant "SALAMI"), and GFZ
684 Potsdam.

685

686 **References**

687

688 Aeschbach-Hertig W., Stute M., Clark J. F., Reuter R. F. and Schlosser P. (2002) A
689 paleotemperature record derived from dissolved noble gases in groundwater of the Aquia
690 Aquifer (Maryland, USA). *Geochim. Cosmochim. Acta* **66**, 797-817.

691

692 Ahonen L., Kietäväinen R., Kortelainen N., Kukkonen I. T., Pullinen A., Toppi T., Bomberg M.,
693 Itävaara M., Nousiainen A., Nyyssönen M. and Öster M. (2011) Hydrogeological characteristics
694 of the Outokumpu Deep Drill Hole. *Geol. Surv. Finl., Spec. Paper* **51**, 151-168.

695

696 Airo M.-L., Säävuori H. and Vuoriainen S. (2011) Petrophysical properties of the Outokumpu
697 deep drill core and the surrounding bedrock. *Geol. Surv. Finl., Spec. Paper* **51**, 63-82.

698

699 Altman S. J., Uchida M., Tidwell V. C., Boney C. M. and Chambers B. P. (2004) Use of X-ray
700 absorption to examine heterogeneous diffusion in fractured crystalline rocks. *J. Contam. Hydrol.*
701 **69**, 1-26.

702

703 Andrews J. N. (1985) The isotopic composition of radiogenic helium and its use to study
704 groundwater movement in confined aquifers. *Chem. Geol.* **49**, 339-351.

Andrews J. N., Giles I. S, Kay R. L. F., Lee D. J., Osmond J. K., Cowart J. B., Fritz P., Barker J. F. and Gale J. (1982) Radioelements, radiogenic helium and age relationships for groundwaters from the granites at Stripa, Sweden. *Geochim. Cosmochim. Acta* **46**, 1533-1543.

Andrews J. N., Hussain N. and Youngman M. J. (1989) Atmospheric and radiogenic gases in groundwaters from the Stripa granite. *Geochim. Cosmochim. Acta* **53**, 1831-1841.

Anell I., Thybo H. and Artemieva I. M. (2009) Cenozoic uplift and subsidence in the North Atlantic region: Geological evidence revisited. *Tectonophysics* **474**, 78-105.

Ballentine C. J. and Burnard P. G. (2002) Production, release and transport of noble gases in the continental crust. *Rev. Mineral. Geochem.* **47**, 481-538.

Ballentine C. J., O'Nions R. K., Oxburgh E. R., Horvath F. and Deak J. (1991) Rare gas constraints on hydrocarbon accumulation, crustal degassing and groundwater flow in the Pannonian Basin. *Earth Planet. Sci. Lett.* **105**, 229-246.

Ballentine C. J., Mazurek M. and Gautschi A. (1994) Thermal constraints on crustal rare gas release and migration: Evidence from Alpine fluid inclusions. *Geochim. Cosmochim. Acta* **58**, 4333-4348.

Ballentine C. J., Burgess R. and Marty B. (2002) Tracing fluid origin, transport and interaction in the crust. *Rev. Mineral. Geochem.* **47**, 539-614.

Blomqvist R. (1999) Hydrogeochemistry of deep groundwaters in the central part of the Fennoscandian Shield. Geol. Surv. Finl., Nuclear Waste Disposal Research, Report YST-101. (http://arkisto.gsf.fi/yst/YST_101.pdf).

734 Bottomley D. J., Ross J. D. and Clarke W. B. (1984) Helium and neon isotope geochemistry of
735 some ground waters from the Canadian Precambrian Shield. *Geochim. Cosmochim. Acta* **48**,
736 1973-1985.
737
738 Bottomley D. J., Gascoyne M. and Kamineni D. C. (1990) The geochemistry, age, and origin of
739 groundwater in a mafic pluton, East Bull Lake, Ontario, Canada. *Geochim. Cosmochim. Acta* **54**,
740 933-1008.
741
742 Castro M. C., Goblet P., Ledoux E., Violette S. and de Marsily G. (1998) Noble gases as natural
743 tracers of water circulation in the Paris Basin 2. Calibration of a groundwater flow model using
744 noble gas isotope data. *Water Resour. Res.* **34**, 2467-2483.
745
746 Claesson S., Huhma H., Kinny P. D. and Williams I. S. (1993) Svecofennian detrital zircon ages
747 – implications for the Precambrian evolution of the Baltic Shield. *Precambrian Res.* **64**, 109-130.
748
749 Clark I. D. and Fritz P. (1997) *Environmental isotopes in hydrogeology*. Lewis Publishers, Boca
750 Raton.
751
752 Clarke W. B., Top Z., Beavan A. P. and Ghandi S. S. (1977) Dissolved helium in lakes: Uranium
753 prospecting in the Precambrian terrain of central Labrador. *Econ. Geol.* **72**, 233-242.
754
755 Clarke W. B., Top Z. and Eismont W. C. (1983) Helium isotope and tritium content of lakes and
756 uranium exploration in the NEA/IAEA Athabasca Test area. In *Uranium Exploration in*
757 *Athabasca Basin, Saskatchewan, Canada* (ed. E. M. Cameron). *Pap. Geol. Surv. Can.* **82-11**,
758 139-146.
759
760 Delos A., Trinchero P., Richard L., Molinero J., Dentz M. and Pitkänen P. (2010) Quantitative
761 assessment of deep gas migration in Fennoscandian sites. SKB R-10-61, Swedish Nuclear Fuel
762 and Waste Management Co (SKB), Stockholm.
763

764 Drescher J., Kirsten T. and Schäfer K. (1998) The rare gas inventory of the continental crust,
765 recovered by the KTB Continental Deep Drilling Project. *Earth Planet. Sci. Lett.* **154**, 247-263.
766
767 Eberhardt P., Eugster O. and Marti K. (1965) A redetermination of the isotopic composition of
768 atmospheric neon. *Z. Naturforsch.* **20a**, 623-624.
769
770 Frape S. K., Fritz P. and McNutt R. H. (1984) Water-rock interaction and chemistry of
771 groundwaters from the Canadian Shield. *Geochim. Cosmochim. Acta* **48**, 1617-1627.
772
773 Frape S. K., Blyth A., Blomqvist R., McNutt R. H. and Gascoyne M. (2003) Deep fluids in the
774 continents: II. Crystalline rocks. In *Surface and ground water, weathering and soils* (ed. J. I.
775 Drever). *Treatise Geochem.* **5**, 541-580.
776
777 Fritz P. and Frape S. K. (1982) Saline groundwaters in the Canadian Shield – a first overview.
778 *Chem. Geol.* **36**, 179-190.
779
780 Gautheron C., Moreira M. and Allègre C. (2005) He, Ne and Ar composition of the European
781 lithospheric mantle. *Chem. Geol.* **217**, 97-112.
782
783 Gilg H. A., Hall A. M., Ebert K. and Fallick A. E. (2013) Cool kaolins in Finland. *Palaeogeogr.,*
784 *Palaeoclimatol., Palaeoecol.* **392**, 454-462.
785
786 Greene S., Battye N., Clark I., Kotzer T. and Bottomley D. (2008) Canadian Shield brine from
787 the Con Mine, Yellowknife, NT, Canada: Noble gas evidence for an evaporated Palaeozoic
788 seawater origin mixed with glacial meltwater and Holocene recharge. *Geochim. Cosmochim.*
789 *Acta* **72**, 4008-4019.
790
791 Greenwood D. R., Basinger J. F. and Smith R. Y. (2010) How wet was the Arctic Eocene rain
792 forest? Estimates of precipitation from Paleogene Arctic macrofloras. *Geology* **38**, 15-18.
793

794 Hall A. M. and Ebert K. (2013) Cenozoic microfossils in northern Finland: Local reworking or
795 distant wind transport? *Palaeogeogr., Palaeoclimatol., Palaeoecol.* **388**, 1-14.
796
797 Haveman S. A., Pedersen K. and Ruotsalainen P. (1999) Distribution and metabolic diversity of
798 microorganisms in deep igneous rock aquifers of Finland. *Geomicrobiol. J.* **16**, 277-294.
799
800 Heinonen S., Kukkonen I. T., Heikkinen P. J. and Schmitt D. R. (2011) High resolution
801 reflection seismics integrated with deep drill hole data in Outokumpu, Finland. *Geol. Surv. Finl.,*
802 *Spec. Paper* **51**, 105-118.
803
804 Hilton D. R. and Craig H. (1989) The Siljan Deep Well: Helium isotope results. *Geochim.*
805 *Cosmochim. Acta* **53**, 3311-3316.
806
807 Holland G., Sherwood Lollar B., Li L., Lacrampe-Couloume G., Slater G. F. and Ballentine C. J.
808 (2013) Deep fracture fluids isolated in the crust since the Precambrian era. *Nature* **497**, 357-360.
809
810 Huhma H. (1986) Sm-Nd, U-Pb and Pb-Pb isotopic evidence for the origin of the early
811 Proterozoic Svecokarelian crust in Finland. *Geol. Surv. Finl., Bull.* **337**, 48 p.
812
813 Itävaara M., Nyyssönen M., Kapanen A., Nousiainen A., Ahonen L. and Kukkonen I. (2011a)
814 Characterization of bacterial diversity to a depth of 1500 m in the Outokumpu deep borehole,
815 Fennoscandian Shield. *FEMS Microbiol. Ecol.* **77**, 295–309.
816
817 Itävaara M., Nyyssönen M., Bomberg M., Kapanen A., Nousiainen A., Ahonen L., Hultman J.,
818 Paulin L., Auvinen P. and Kukkonen I. T. (2011b) Microbiological sampling and analysis of the
819 Outokumpu Deep Drill Hole biosphere in 2007-2009. *Geol. Surv. Finl., Spec. Pap.* **51**, 199-206.
820
821 Kennedy B. M., Hiyagon H. and Reynolds J. H. (1990) Crustal neon: a striking uniformity. *Earth*
822 *Planet. Sci. Lett.* **98**, 277-286.
823

824 Kietäväinen R., Ahonen L., Kukkonen I. T., Hendriksson N., Nyyssönen M. and Itävaara M.
825 (2013) Characterisation and isotopic evolution of saline waters of the Outokumpu Deep Drill
826 Hole, Finland – Implications for water origin and deep terrestrial biosphere. *Appl. Geochem.* **32**,
827 37-51.
828
829 Kipfer R., Aeschbach-Hertig W., Peeters F. and Stute M. (2002) Noble gases in lakes and ground
830 waters. *Rev. Mineral. Geochem.* **47**, 615-700.
831
832 Kloppmann W., Girard J.-P. and Négrel P. (2002) Exotic stable isotope compositions of saline
833 waters and brines from the crystalline basement. *Chem. Geol.* **184**, 49-70.
834
835 Kohonen J. and Rämö O. T. (2005) Sedimentary rocks, diabases, and late cratonic evolution. In
836 *Precambrian Geology of Finland – Key to evolution of the Fennoscandian Shield* (eds. M.
837 Lehtinen, P. Nurmi and O. T. Rämö). Elsevier, Amsterdam. pp. 563-604.
838
839 Korsman K., Korja T., Pajunen M., Virransalo P. and GGT/SVEKA Working Group (1999) The
840 GGT/SVEKA Transect: Structure and evolution of the continental crust in the Paleoproterozoic
841 Svecofennian orogen in Finland. *Int. Geol. Rev.* **41**, 287-333.
842
843 Kukkonen I. T., Rath V., Kivekäs L., Šafanda J. and Čermák V. (2011) Geothermal studies of
844 the Outokumpu Deep Drill Hole, Finland: Vertical variation in heat flow and palaeoclimatic
845 implications. *Phys. Earth Planet. Inter.* **188**, 9-25.
846
847 Kukkonen I. T., Heinonen S., Heikkinen P. and Sorjonen-Ward P. (2012) Delineating ophiolite-
848 derived host rocks of massive sulfide Cu-Co-Zn deposits with 2D high resolution seismic
849 reflection data in Outokumpu, Finland. *Geophysics* **77**, WC213-WC222.
850
851 Kulongoski J. T., Hilton D. R. and Izbicki J. A. (2005) Source and movement of helium in the
852 eastern Morongo groundwater Basin: The influence of regional tectonics on crustal and mantle
853 helium fluxes. *Geochim. Cosmochim. Acta* **69**, 3857-3872.
854

Lahtinen R., Huhma H., Kontinen A., Kohonen J. and Sorjonen-Ward P. (2010) New constraints for the source characteristics, deposition and age of the 2.1-1.9 Ga metasedimentary cover at the western margin of the Karelian Province. *Precambrian Res.* **176**, 77-93.

Larsson L. M., Dybkjær K., Rasmussen E. S., Piasecki S., Utescher T. and Vajda V. (2011) Miocene climate evolution of northern Europe: A palynological investigation from Denmark. *Palaeogeogr., Palaeoclimatol., Palaeoecol.* **309**, 161-175.

Lee J.-Y., Marti K., Severinghaus J. P., Kawamura K., Yoo H.-S., Lee J. B. and Kim J. S. (2006) A redetermination of the isotopic abundances of atmospheric Ar. *Geochim. Cosmochim. Acta* **70**, 4507-4512.

Lin L.-H., Wang P.-L., Rumble D., Lippmann-Pipke J., Boice E., Pratt L. M., Sherwood Lollar B., Brodie E. L., Hazen T. C., Andersen G. L., DeSantis T. Z., Moser D.P., Kershaw D. and Onstott T. C. (2006) Long-term sustainability of a high-energy, low-diversity crustal biome. *Science* **314**, 479-482.

Lippmann J., Stute M., Torgersen T., Moser D. P., Hall J. A., Lin L., Borcsik M., Bellamy R. E. S. and Onstott T. C. (2003) Dating ultra-deep mine waters with noble gases and ^{36}Cl, Witwatersrand Basin, South Africa. *Geochim. Cosmochim. Acta* **67**, 4597-4619.

Lippmann J., Erzinger J., Zimmer M., Schloemer S., Eichinger L. and Faber E. (2005) On the geochemistry of gases and noble gas isotopes (including ^{222}Rn) in deep crustal fluids: the 4000 m KTB-pilot hole fluid production test 2002–03. *Geofluids* **5**, 52-66.

Lippmann-Pipke J., Sherwood Lollar B., Niedermann S., Stroncik N. A., Naumann R., van Heerden E. and Onstott T. C. (2011) Neon identifies two billion year old fluid component in Kaapvaal Craton. *Chem. Geol.* **283**, 287-296.

Louvat D., Michelot J.L. and Aranyossy J. F. (1999) Origin and residence time of salinity in the Äspö groundwater system. *Appl. Geochem.***14**, 917-925.

Mamyrin B. A., Anufriyev G. S., Kamenskiy I. L. and Tolstikhin I. N. (1970) Determination of the isotopic composition of atmospheric helium. *Geochem. Int.* **7**, 498-505.

Marty B. (1984) On the noble gas isotopic fractionation in naturally occurring gases. *Geochem. J.* **18**, 157-162.

Matsumoto T., Honda M., McDougall I., Yatsevich I. and O'Reilly S. Y. (2004) Isotope fractionation of neon during stepheating extraction? A comment of 'Re-interpretation of the existence of a primitive plume under Australia based on neon isotope fractionation during step heating' by Gautheron and Moreira (2003). *Terra Nova* **16**, 23-26.

Moreira M., Kunz J. and Allègre C. (1998) Rare gas systematics in popping rock: Isotopic and elemental compositions in the upper mantle. *Science* **279**, 1178-1181.

Moser D. P., Onstott T. C., Fredrickson J. K., Brockman F. J., Balkwill D. L., Drake G. R., Pfiffner S. M. and White D. C. (2003) Temporal shifts in the geochemistry and microbial community structure of an ultradeep mine borehole following isolation. *Geomicrobiol. J.* **20**, 517-548.

Neretnieks I. (2013) Some aspects of release and transport of gases in deep granitic rocks: possible implications for nuclear waste repositories. *Hydrogeol. J.* **21**, 1701-1716.

Niedermann S., Bach W. and Erzinger J. (1997) Noble gas evidence for a lower mantle component in MORBs from the southern East Pacific Rise: Decoupling of helium and neon isotope systematics. *Geochim. Cosmochim. Acta* **61**, 2697-2715.

Nier A. O. (1950) A redetermination of the relative abundances of the isotopes of neon, krypton, rubidium, xenon, and mercury. *Phys. Rev.* **79**, 450-454.

916 Nurmi P. A. and Kukkonen I. T. (1986) A new technique for sampling water and gas from deep
917 drill holes. *Can. J. Earth Sci.* **23**, 1450-1454.
918
919 Nurmi P. A., Kukkonen I. T. and Lahermo P. W. (1988) Geochemistry and origin of saline
920 groundwaters in the Fennoscandian Shield. *Appl. Geochem.* **3**, 185-203.
921
922 Nyyssönen M., Hultman J., Ahonen L., Kukkonen I., Paulin L., Laine P., Itävaara M. and
923 Auvinen P. (2014) Taxonomically and functionally diverse microbial communities in deep
924 crystalline rocks of the Fennoscandian shield. *ISME J.* **8**, 126-138.
925
926 Peltonen P., Kontinen A., Huhma H. and Kuronen U. (2008) Outokumpu revisited: New mineral
927 deposit model for the mantle peridotite-associated Cu-Co-Zn-Ni-Ag-Au sulphide deposits. *Ore*
928 *Geol. Rev.* **33**, 559-617.
929
930 Piribauer C. J., Sindern S., Meyer F. M., Vennemann T. W. and Prochaska W. (2011) Fluid
931 inclusions in the Outokumpu Deep Drill Core: Implications for palaeofluid evolution and the
932 composition of modern deep saline fluids. *Geol. Surv. Finl., Spec. Paper* **51**, 169-180.
933
934 Purkamo L., Bomberg M., Nyyssönen M., Kukkonen I., Ahonen L., Kietäväinen R. and Itävaara
935 M. (2013) Dissecting the deep biosphere: retrieving authentic microbial communities from
936 packer-isolated deep crystalline bedrock fracture zones. *FEMS Microbiol. Ecol.* **85**, 324-337.
937
938 Regenspurg S., Wiersberg T., Brandt W., Huenges E., Saadat A., Schmidt K. and Zimmermann
939 G. (2010) Geochemical properties of saline geothermal fluids from the in-situ geothermal
940 laboratory Groß Schönebeck (Germany). *Chem. Erde* **70**, 3-12.
941
942 Säntti J., Kontinen A., Sorjonen-Ward P., Johanson B. and Pakkanen L. (2006) Metamorphism
943 and chromite in serpentinized and carbonate-silica-altered peridotites of the Paleoproterozoic
944 Outokumpu-Jormua Ophiolite Belt, eastern Finland. *Int. Geol. Rev.* **48**, 494-546.
945

946 Sherwood Lollar B., Frape S. K., Weise S. M., Fritz P., Macko S. A. and Welhan J. A. (1993)
947 Abiogenic methanogenesis in crystalline rocks. *Geochim. Cosmochim. Acta* **57**, 5087-5097.
948
949 Steffen H. and Wu P. (2011) Glacial isostatic adjustment in Fennoscandia – A review of data and
950 modeling. *J. Geodyn.* **52**, 169-204.
951
952 Steiger R. H. and Jäger E. (1977) Subcommission on geochronology: Convention on the use of
953 decay constants in geo- and cosmochronology. *Earth Planet. Sci. Lett.* **36**, 359-362.
954
955 Tolstikhin I., Lehmann B. E., Loosli H. H. and Gautschi A. (1996) Helium and argon isotopes in
956 rocks, minerals, and related groundwaters: A case study in northern Switzerland. *Geochim.*
957 *Cosmochim. Acta* **60**, 1497-1514.
958
959 Top Z. and Clarke W. B. (1981) Dissolved helium isotopes and tritium in lakes: Further results
960 for uranium prospecting in central Labrador. *Econ. Geol.* **76**, 2018-2031.
961
962 Torgersen T. (1980) Controls on pore-fluid concentration of ^{4}He and ^{222}Rn and the calculation of
963 ^{4}He/^{222}Rn ages. *J. Geochem. Explor.* **13**, 57-75.
964
965 Torgersen T. (1989) Terrestrial helium degassing fluxes and the atmospheric helium budget:
966 Implications with respect to the degassing processes of continental crust. *Chem. Geol.* **79**, 1-14.
967
968 Torgersen T. (2010) Continental degassing flux of ^{4}He and its variability. *Geochem. Geophys.*
969 *Geosyst.* **11**, Q06002, doi: 10.1029/2009GC002930.
970
971 Torgersen T. and Clarke W. B. (1985) Helium accumulation in groundwater, I: An evaluation of
972 sources and the continental flux of crustal ^{4}He in the Great Artesian Basin, Australia. *Geochim.*
973 *Cosmochim. Acta* **49**, 1211-1218.
974
975 Torgersen T. and Ivey G. N. (1985) Helium accumulation in groundwater, II: A model for the
976 accumulation of the crustal ^{4}He degassing flux. *Geochim. Cosmochim. Acta* **49**, 2445-2452.

977

978 Torsvik T. H., Van der Voo R., Meert J. G., Mosar J. and Walderhaug H. J. (2001)
979 Reconstructions of the continents around the North Atlantic at about the 60th parallel. *Earth*
980 *Planet. Sci. Lett.* **187**, 55-69.
981
982 Tynni R. (1982) The reflection of geological evolution in Tertiary and interglacial diatoms and
983 silicoflagellates in Finnish Lapland. *Geol. Surv. Finl., Bull.* **320**, 40 p.
984
985 Västi K. (2011) Petrology of the drill hole R2500 at Outokumpu, eastern Finland – the deepest
986 drill hole ever drilled in Finland. *Geol. Surv. Finl., Spec. Paper* **51**, 17-46.
987
988 Yatsevich I. and Honda M. (1997) Production of nucleogenic neon in the Earth from natural
989 radioactive decay. *J. Geophys. Res.* **102**, 10,291–10,298.
990
991 Zachos J., Pagani M., Sloan L., Thomas E. and Billups K. (2001) Trends, rhythms, and
992 aberrations in global climate 65 Ma to present. *Science* **292**, 686-693.
993

Figure captions

Fig. 1. Lithology (a) of the Outokumpu region and (b) along the Outokumpu Deep Drill Hole. The uppermost 30 m of the profile comprise Quaternary sand and silt (not shown in the legend). Arrows indicate the main points in which density difference driven flow into (arrows pointing left) and out (arrows pointing right) of the drill hole, originating from mixing between saline formation fluids and residual drilling water, has been observed. Hydraulic conductivities, measured during drilling, are from Ahonen et al. (2011) and division into different water types from Kietäväinen et al. (2013). Modified after Kukkonen et al. (2012) and Kietäväinen et al. (2013).

Fig. 2. Vertical variation of (a) He and (b) Ar concentrations before and after correction for air-contamination (open and filled symbols, respectively) and of (c) $^{3}He/^{4}He$ and (d) $^{40}Ar/^{36}Ar$ ratios along the Outokumpu Deep Drill Hole. The air-contamination correction in (a) and (b) is based on the assumption that all O_2 is of atmospheric origin (Eqs. 1 and 2). Atmospheric ratio of $^{40}Ar/^{36}Ar$ (Lee et al. 2006) is indicated with a dashed line. Symbols in (c) and (d) are coded according to the sample type: diamond = sampling bulb gas, square = Cu-tube gas and triangle = Cu-tube water.

Fig. 3. Three-isotope plot for Ne. Symbols as in Fig. 2c and d. MFL = mass fractionation line for air (see Eq. 7). Composition of air is from Eberhardt et al. (1965). The air-crust mixing line is calculated using a crustal end member composition with $^{21}Ne/^{22}Ne = 0.47$ and $^{20}Ne/^{22}Ne = 0$ (Kennedy et al. 1990). The air-mantle (MORB) mixing line is calculated using $^{21}Ne/^{22}Ne = 13.8$ and $^{20}Ne/^{22}Ne = 0.075$ (Moreira et al. 1998). Also indicated is the potential air-Archaean Ne mixing line with $^{21}Ne/^{22}Ne = 3.3$ and $^{20}Ne/^{22}Ne = 0$ (Lippmann-Pipke et al. 2011).

Fig. 4. *In situ* noble gas residence times and salinity expressed as total dissolved solids (TDS) along the Outokumpu Deep Drill Hole. The TDS values (dashed line) are from Kietäväinen et al. (2013).

Fig. 5. Diffusion of He in crystalline bedrock. The one-dimensional model according to Andrews (1985) is based on a porosity of 0.5 % and uniform distribution of U and Th with a He diffusion coefficient of $3.18 \cdot 10^{-9}$ cm^2 s^{-1}. In addition to modelled profiles, samples from 2011 described in this study (squares), the average of three samples from 180 m depth taken with a pressurised sampling device (PAVE) in 2012 after 45 days of pumping between packers (triangle), and one sample taken from around 977 m depth during drilling in 2004 (circle) are shown.

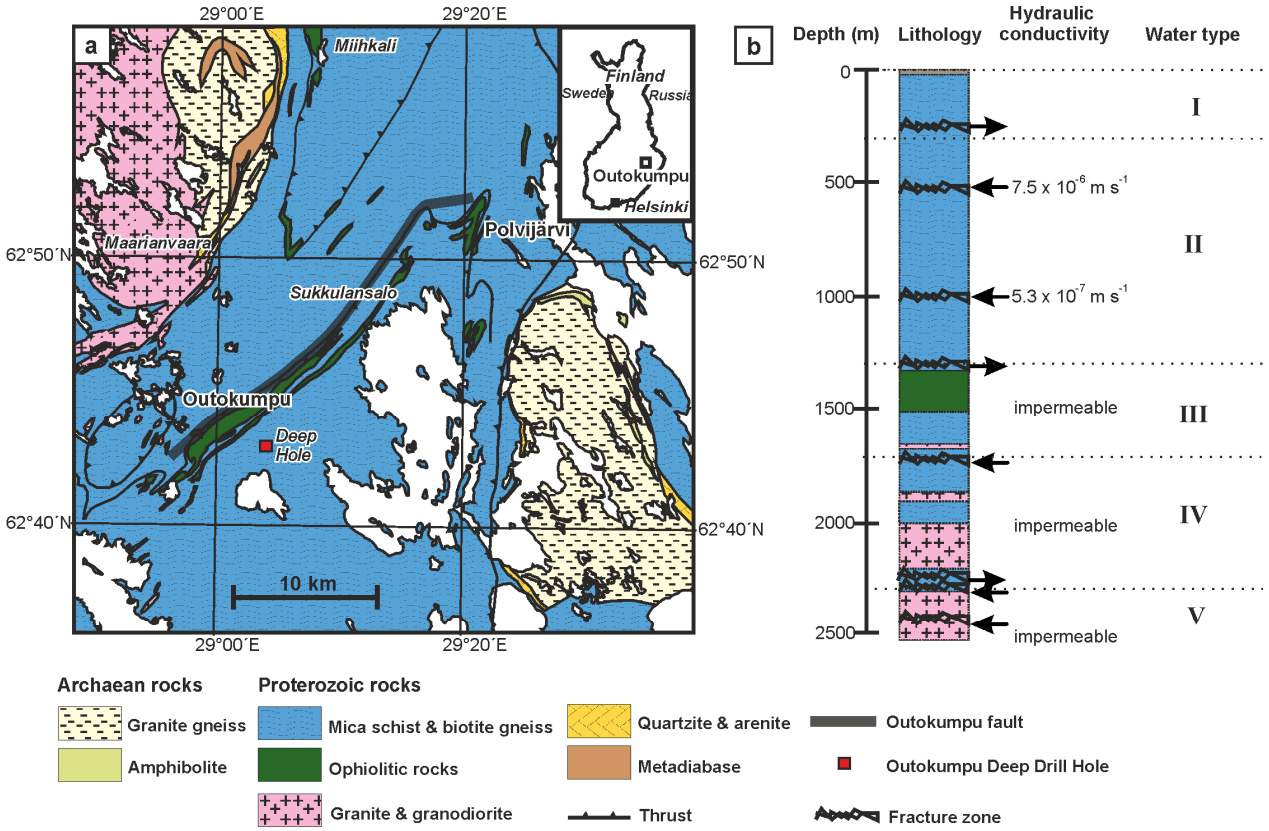
a
29°00´E
29°20´E
62°50´N
62°40´N
Miihkali
Maarianvaara
Sukkulansalo
Outokumpu
Deep Hole
Polvijärvi
10 km
Finland
Sweden
Russia
Helsinki
b
Depth (m)
Lithology
Hydraulic conductivity
Water type
0
500
1000
1500
2000
2500
7.5 x 10-6 m s-1
5.3 x 10-7 m s-1
impermeable
impermeable
impermeable
I
II
III
IV
V
Archaean rocks
Granite gneiss
Amphibolite
Proterozoic rocks
Mica schist & biotite gneiss
Ophiolitic rocks
Granite & granodiorite
Quartzite & arenite
Metadiabase
Thrust
Outokumpu fault
Outokumpu Deep Drill Hole
Fracture zone

Figure 1

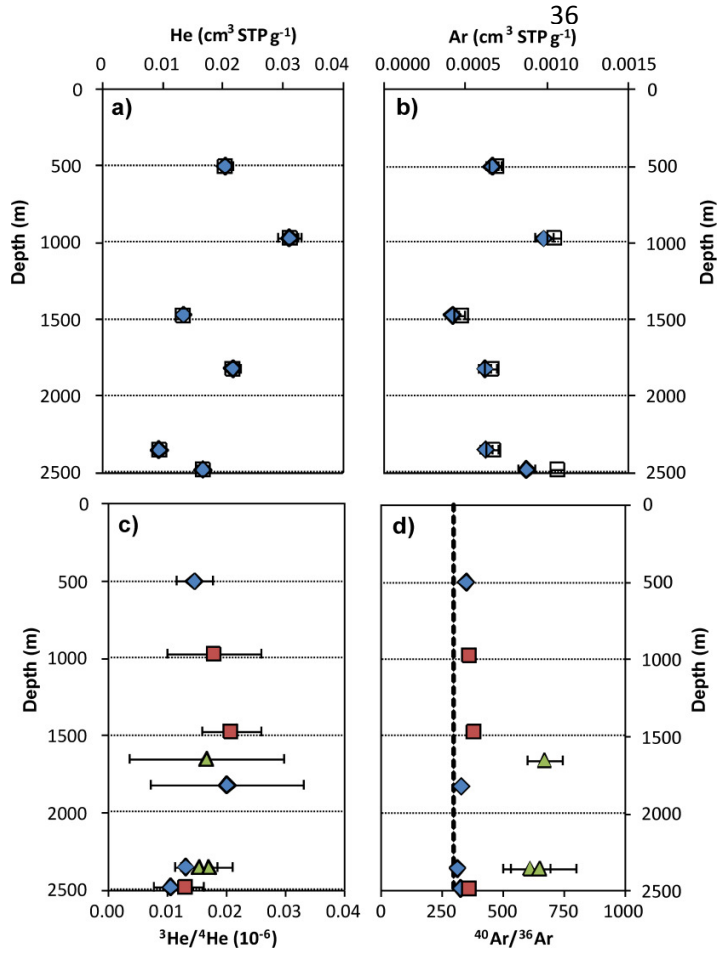

Figure 2

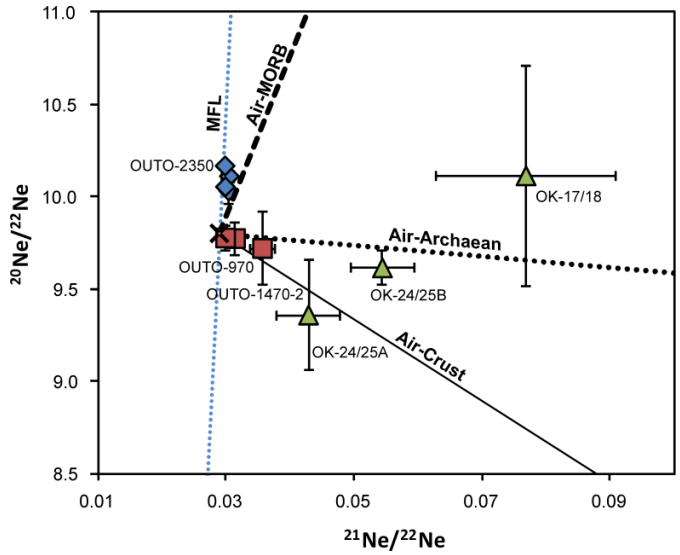

Figure 3

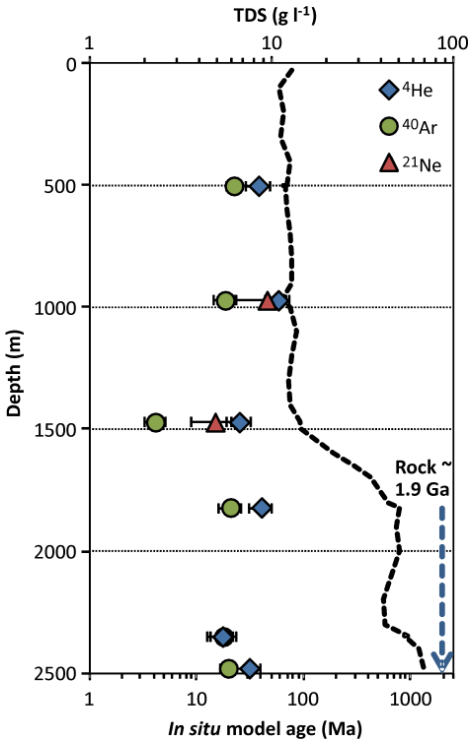

Figure 4

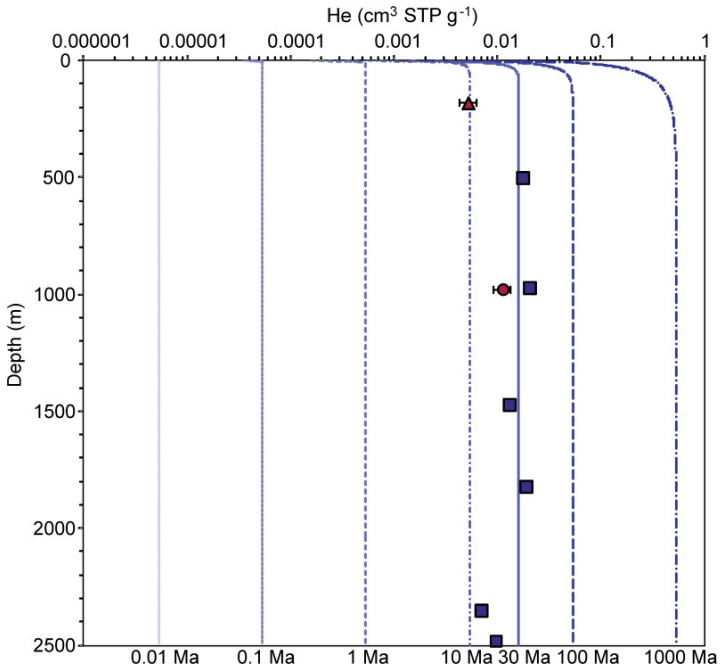

Figure 5

Table 1

Characteristics of the bedrock at Outokumpu.

Water type[a]	Depth (m)	Main rock type	ρ_r[b] ($g\ cm^{-3}$)		Porosity[b]				U_{rock} (ppm)[c]				Th_{rock} (ppm)[c]				K_{rock} (%)[c]			
				2σ	Min	Max	Mean	2σ	Min	Max	Mean	2σ	Min	Max	Mean	2σ	Min	Max	Mean	2σ
I	0 - 300	Mica schist	2.742	0.006	0.0007	0.0161	0.0037	0.0008	2.8	3.8	3.1	0.5	9.8	12.2	10.9	1.3	1.3	3.4	2.6	1.1
II	300 - 1300	Mica schist	2.746	0.002	0.00020	0.01580	0.00320	0.00011	1.9	4.9	3.0	0.3	7.5	16.1	9.0	0.7	0.7	6.3	2.3	0.4
III	1300 - 1700	Ophiolitic rocks	2.750	0.015	0.0010	0.0725	0.0106	0.0014	<0.2	30	8	2	<0.5	11.8	7.0	1.0	0.003	4.3	0.7	0.3
IV	1700 - 2300	Mica schist	2.703	0.006	0.0019	0.0228	0.0057	0.0003	2.4	25	10	4	2	31	11	3	0.6	5.4	2.6	0.7
V	2300 - 2516	Pegmatite	2.654	0.016	0.0023	0.0122	0.0049	0.0006	2.2	15	6	7	7	24	13	9	0.6	2.0	1.3	0.8
All	0 - 2516	Mica schist	2.730	0.004	0.0002	0.0725	0.0053	0.0003	<0.2	29.7	6.5	1.4	<0.5	30.5	9.4	0.9	0.003	6.3	1.6	0.3

[a]Kietäväinen et al. (2013)

[b]Airo et al. (2011); mean values with n= 87, 891, 352, 518, 62, and 1910 for sections I, II, III, IV, V, and "All", respectively.

[c]Västi (2011), mean values with n= 4, 28, 47, 18, 4 and 101 for sections I, II, III, IV, V, and "All", respectively.

Table 2

Gas compositions (cm^3 STP g^{-1}) in the Outokumpu Deep Drill Hole groundwater measured with a quadrupole mass spectrometer and corrected for air-contamination. Last column shows the amount of O_2 on which the correction was based. A 2σ uncertainty of 6 % applies for all corrected values and 4 % for O_2.

	Depth	CH_4	N_2	He	Ar	H_2	CO_2	O_2
	m				10^{-3}	10^{-3}	10^{-3}	vol-%
OUTO-500-2	500	0.50	0.174	0.0203	0.66	0.58	0.104	0.078
OUTO-970	970	0.77	0.272	0.0310	0.98	0.80	0.169	0.130
OUTO-1470-2	1470	0.173	0.047	0.0134	0.42	0.12	0.031	0.53
OUTO-1820	1820	0.45	0.071	0.0216	0.62	26.2	0.090	0.150
OUTO-2350	2350	0.0261	0.030	0.0094	0.62	18.5	0.021	1.15
OUTO-2480	2480	0.051	0.036	0.0166	0.87	35	0.147	2.60

Table 3

Measured noble gas isotope ratios and calculated abundances (in cm^3 STP g^{-1}) of nucleogenic ^{21}Ne (Eq. 5) and radiogenic ^{40}Ar (Eq. 6) in the Outokumpu Deep Drill Hole fluids. All errors are 2σ.

Sample	Type	Depth	$^3He/^4He$		$^{20}Ne/^{22}Ne$		$^{21}Ne/^{22}Ne$		$^{40}Ar/^{36}Ar$		$^{38}Ar/^{36}Ar$		$^{134}Xe/^{132}Xe$		$^{136}Xe/^{132}Xe$		$^4He/^{20}Ne$		$^{21}Ne_{nucl}$		$^{40}Ar_{rad}$	
		m	(10^{-6})	±		±		±		±		±		±		±		±	(10^{-9})	±	(10^{-3})	±
OUTO-500-2	Cu-tube gas	500	0.015	0.003	10.11	0.03	0.0304	0.0005	349.4	1.3	0.1856	0.0007	0.39	0.04	0.34	0.04	2100	100			0.73	0.05
OUTO-970 [a]	*Cu-tube gas*	*970*	*0.20*	*0.15*	*9.85*	*0.03*	*0.0285*	*0.0006*	*298*	*4*	*0.1873*	*0.0009*	*0.396*	*0.007*	*0.329*	*0.008*	*2.30*	*0.17*				
OUTO-970	Sampling bulb gas	970	0.018	0.008	9.78	0.09	0.0314	0.0010	362	5	0.1878	0.0012	0.40	0.03	0.35	0.03	7100	540	1.1	0.5	0.60	0.07
OUTO-1470-2 [a]	*Cu-tube gas*	*1470*	*0.019*	*0.006*	*9.94*	*0.04*	*0.0292*	*0.0011*	*296*	*3*	*0.1862*	*0.0013*	*0.39*	*0.02*	*0.34*	*0.03*	*81*	*6*				
OUTO-1470-2	Sampling bulb gas	1470	0.021	0.005	9.7	0.2	0.036	0.002	381	5	0.1879	0.0016	0.40	0.06	0.34	0.03	26,000	2000	0.36	0.12	0.134	0.014
OK-17/18	Cu-tube water	1650	0.017	0.013	10.1	0.6	0.077	0.014	670	70	0.189	0.003	0.40	0.08	0.35	0.04	40,000	16,000				
OUTO-1820	Cu-tube gas	1820	0.020	0.013	10.03	0.07	0.0303	0.0010	329	4	0.1849	0.0012	0.40	0.03	0.34	0.03	1500	110			0.67	0.11
OUTO-2350	Cu-tube gas	2350	0.013	0.002	10.17	0.02	0.0298	0.0004	313	3	0.1850	0.0014	0.40	0.02	0.34	0.03	420	20			0.58	0.14
OK-24/25/A	Cu-tube water	2350	0.015	0.003	9.4	0.3	0.043	0.005	610	80	0.1888	0.0015	0.41	0.02	0.37	0.02	40,000	13,000				
OK-24/25/B [b]	Cu-tube water	2350	0.017	0.004	9.62	0.09	0.054	0.005	650	150	0.1878	0.0016	0.42	0.03	0.363	0.018	65,000	13,000				
OUTO-2480	Cu-tube gas	2480	0.011	0.003	10.06	0.03	0.0298	0.0005	327	2	0.1854	0.0015	0.415	0.009	0.370	0.007	660	40			1.18	0.14
OUTO-2480	Sampling bulb gas	2480	0.013	0.003	9.78	0.07	0.0298	0.0010	361.9	1.4	0.1879	0.0010	0.413	0.006	0.360	0.009	4100	300			0.54	0.05
Air [c]			1.39		9.80		0.029		298.56		0.1885		0.3879		0.3294		0.319					

[a] Samples in *italics* show massive contamination with atmospheric air, and have been excluded from the residence time calculations.

[b] After active degassing by ultrasonic agitation.

[c] Values are according to Nier (1950) for Xe, Eberhardt et al. (1965) for Ne, Mamyrin et al. (1970) for He and Lee et al. (2006) for Ar.

Table 4

Noble gas residence times (Ma) in the Outokumpu Deep Drill Hole groundwater calculated according to *in situ* model, with 2σ uncertainties. Parameters used in the calculation are presented in Table 1 ("All").

		In situ model age					
Sample	Depth	^{4}He		^{21}Ne		^{40}Ar	
	(m)		±		±		±
OUTO-500-2	500	38	9			22	3
OUTO-970	970	58	14	45	22	18	4
OUTO-1470-2	1470	25	6	15	6	4.1	0.9
OUTO-1820	1820	40	10			21	5
OUTO-2350	2350	17	4			18	5
OUTO-2480	2480	31	8			20	3